Supporting Information for "The presence of Africa and limited soil moisture contribute to future drying of South America"

M. Pietschnig[1], F. H. Lambert[1], M. Saint-Lu[2]and G. K. Vallis[1]

[1]Department of Mathematics, University of Exeter, Exeter, United Kingdom

[2]Laboratoire de Météorologie Dynamique (LMD) / Institut Pierre Simon Laplace (IPSL), Sorbonne Université, Université Pierre et Marie Curie, Paris, France

Contents of this file

1. Text S1 to S9
2. Figures S1 to S9

Introduction

The supplementary material contains nine figures and texts as additional information for the main text.

Text S1.

Figure S1a shows ΔP and $(P-E)_{ctl}$ (contours) with global warming for the realistic continents with topography and bucket model (in analogy to Figure 1a in the main text). Instead of prescribing sea surface temperatures, we have parameterized the ocean heat

transport based on AMIP SSTs (Vallis et al., 2018). This allows us to use a mixed-layer ('slab') ocean of 20 m depth, and thus for ocean temperatures to adapt freely to climate forcing (in this case a doubling of CO_2), albeit the ocean heat transport parameterization remains unchanged with warming. This results in ΔSST patterns which roughly resemble those projected by coupled models (e.g. Chadwick et al., 2017). We wish to show here that even if we include ΔSST patterns and pattern changes, we obtain a similar $(P-E)_{ctl}$ and ΔP distribution compared to the RC experiment (with prescribed zonally uniform SSTs). Thus, ΔP does not appear to be too sensitive to ΔSST patterns in Isca. We therefore deem our method – prescribing zonally uniform SSTs and globally uniform ocean warming of 2.5 K – suitable for studying ΔP in the tropics.

Text S2.

Figure S2 is supplementary to Figure 1a from the main text showing the same ΔP, but here we have included stippling to show the regions where ΔP exceeds the natural variability (p-value < 0.05 in Welch's t-test, i.e. we can reject the 'null-hypothesis' that the time-series of control and perturbed annual mean precipitation have the same mean). In accordance with ΔP projections from CMIP5 (multi-model mean for the RCP8.5 scenario comparing 1986-2005 to 2081-2100, IPCC (2013)[Fig. SPM.8 b, right panel]), ΔP over Equatorial and South Africa exceeds the natural variability. Over South America, ΔP only exceeds the natural variability in a few locations around the Equator in our study. In CMIP5, ΔP does exceed natural variability over most of the Amazon, but P changes over tropical land are generally quite uncertain concerning agreement among the models (IPCC (2013), Kooperman et al. (2018)[Supplementary Table S2]).

The CMIP5 (RCP8.5 scnenario, comparing the end to the beginning of the 21st century) multi-model mean, annual mean ΔP for the Amazon basin is -0.39 mm/day and 0.16 mm/day for tropical Africa (Kooperman et al., 2018)[Supplementary Table S1]. In the same regions as defined in Kooperman et al. (2018), the estimates from our RC experiment are 0.24 mm/day for the Amazon basin and 0.43 mm/day for tropical Africa. Note that the CO_2 concentration increases from roughly 350 ppm to 950 ppm in Kooperman et al. (2018) and the estimates are multi-model means, whereas our simulations are based on a doubling of CO_2 from 300 ppm to 600 ppm in a single model. Similar to our estimates, some of the CMIP5 models also predict an increase in precipitation averaged over the Amazon region and a stronger increase over tropical Africa, such as IPSL-CM5A-LR, MIROC-ESM and CMCC-CESM (Kooperman et al., 2018)[Supplementary Table S2], albeit the numbers are not directly comparable to our estimates due to the stronger forcing in CMIP5, as discussed above.

Text S3.

Figure S3 shows what would happen if the annual mean SST maximum were located at the Equator for the realistic continents and the idealized two continents. In both cases, the continental precipitation response is generally weaker compared to the experiments where the annual mean SST maximum is North of the Equator (RC and 2C in the main text). Interestingly, this hemispherically symmetric set-up leads to a more widespread increase in P over the Amazon basin in the realistic case. In the idealized simulation, precipitation increases along the Equator over America, and the decrease in the subtropics is much weaker compared to 2C from the main text. Both experiments suggest that the drying

over the Amazon region could be connected to the displacement of the SST maximum to the North of the Equator in the real world.

Text S4.

Figure S4 shows the precipitation change with warming in an experiment where idealized America covers only the latitudinal band from 30°S to 10°N. This set-up is not hemispherically symmetric which adds another level of complexity to the simulation, but is closer to realistic continents. We find that the patterns of ΔP over America are generally similar to our original set-up, albeit the P increase along the Equator is more widespread and there is less drying south of the Equator compared to experiment 2C. However, our original set-up is preferable in order to keep the experimental design as simple as possible, but as complex as necessary.

Text S5.

Figure S5 is supplementary to Fig. 2d in the main text. It shows the difference in ΔP for both idealized continents minus Africa alone (2C-AF). This shows the impact of America on Africa, rather than the impact of Africa on America (as in Fig. 2d in the main text). The fact that the drying impact of Africa on America is larger than the other way around has been explained for the present-day climate (Cook et al., 2004): The anomalous ascent over the continent leads to descent primarily to the west of the continent. The authors explained that the heating-induced low-level convergence over the continent leads to deceleration of the easterlies on the west side of the continent. This reduces wind speeds and surface heat fluxes, leading to a cooler lower atmosphere and favorable conditions for descent. To the east of the continent, the prevailing easterly winds are enhanced by the

low-level convergence towards the continent. This leads to stronger heating of the lower atmosphere through surface heat fluxes and thus unfavorable conditions for subsidence to the east of the continent.

Text S6.

Figure S6 is a supplement to Figure 3 in the main text, showing the Matsuno-Gill-like circulation enhancement with warming due to the presence of Africa (2C - AM). Warming-induced changes in the geopotential height (Δgph) of the 870 hPa and 200 hPa pressure surfaces are shown. Blue is a decrease, red an increase in the gph. The vectors show changes in the horizontal wind field, roughly following geostrophic balance. We find a very clear increase in the Rossby-wave response over the African continent (Gill, 1980). The Rossby-wave response consists of a (weak) cyclone pair near the surface, and a strong anti-cyclone pair aloft.

Text S7.

Figure S7 shows the vertical profile of Δq, and the same changes in the zonal and vertical winds as in Figure 3 in the main text. Panels a) - c) are for each idealized continental configuration: a) AM, b) AF, c) 2C and d) highlights the impact that circulation changes over Africa have on America. In all three cases (a - c), the specific humidity increases everywhere, but d) shows that the increase in q over America and the Atlantic Ocean is smaller in the simulation with both continents (c) compared to the simulation with America only (a). This indicates that – due to the anomalous subsidence caused by enhanced ascent over Africa – the air close to the surface is drier over the Atlantic Ocean

than in the absence of Africa. This drier air is then advected onto the American continent, ultimately resulting in a decrease in precipitation with warming.

Text S8.

Figure S8 demonstrates the high correlation of precipitation, surface temperature and evaporation with surface relative humidity for the land regions in the perturbed 2C experiment. Regions with high P and E also have high r_s. In contrast, T_S and r_S are negatively correlated: Surface temperatures are highest in regions of low surface relative humidity and little rainfall (brown points). Lower temperatures are associated with high precipitation (turquoise points) and high r_S.

Text S9.

Using the fact that $r_{S,ctl}$ is close to a single-valued function of $T_{S,ctl}$, we estimate $g = \frac{dr_{S,ctl}}{dq_{S,ctl}}$ from all tropical land points in the control climate. We can then calculate the Δr_S that would be expected to occur from Δq_S as $\Delta r_S \sim g\Delta q_S$. ΔP follows from Δr_S with Equation 3 from the main text. This prediction does not take the tropics-wide reductions in land r_S into account, which will occur as land warms with respect to ocean (Joshi et al., 2008). However, for compatibility with Equation 3 in the main text it is sufficient to capture changes in r_S with respect to other land regions. Figure S9a is a reconstruction of Δr_S from $g\Delta q_S$, showing that we can derive Δr_S over tropical land reasonably well from Δq_S and the relationship between these two variables in the control climate (g). In contrast, using Δq_{TH} to reconstruct Δr_S (panel b) produces marked degradation, particularly over Africa. Over this continent, Δq_{TH} predicts small changes in r_S with respect to the land mean where the model simulations show substantial increases. Δr_S

over America is better predicted by Δq_{TH}, but this is not true for ΔP_{pred} as discussed in the main text. This occurs because it is the r_S value with respect to the tropical land mean that is associated with ΔP.

References

Chadwick, R., Douville, H., & Skinner, C. B. (2017). Timeslice experiments for understanding regional climate projections: applications to the tropical hydrological cycle and European winter circulation. *Climate Dynamics*, *49*(9). doi: 10.1007/s00382-016-3488-6

Cook, K. H., Hsieh, J.-S., & Hagos, S. M. (2004). The Africa-South America Intercontinental Teleconnection. *Journal of Climate*, *17*(14), 2851-2865. doi: 10.1175/1520-0442(2004)017⟨2851:TAAIT⟩2.0.CO;2

Gill, A. E. (1980). Some simple solutions for heat-induced tropical circulation. *Quarterly Journal of the Royal Meteorological Society*, *106*(449), 447-462. doi: 10.1002/qj.49710644905

IPCC. (2013). *Summary for Policymakers. In: Climate Change 2013: The Physical Science Basis.Contribution of Working Group I to the Fifth Assessment Report of the Intergovernmental Panel on Climate Change [Stocker, T.F., D. Qin, G.-K. Plattner, M. Tignor, S.K. Allen, J. Boschung, A. Nauels, Y. Xia, V. Bex and P.M. Midgley (eds.)]. Cambridge University Press, Cambridge, United Kingdom and New York, NY, USA.*

Joshi, M. M., Gregory, J. M., Webb, M. J., Sexton, D. M. H., & Johns, T. C. (2008, Apr). Mechanisms for the land/sea warming contrast exhibited by simulations of climate

change. *Climate Dynamics*, *30*(5), 455–465. doi: 10.1007/s00382-007-0306-1

Kooperman, G. J., Chen, Y., Hoffman, F. M., Koven, C. D., Lindsay, K., Pritchard, M. S., ... Randerson, J. T. (2018). Forest response to rising CO2 drives zonally asymmetric rainfall change over tropical land. *Nature Climate Change*, *8*. doi: 10.1038/s41558-018-0144-7

Vallis, G. K., Colyer, G., Geen, R., Gerber, E., Jucker, M., Maher, P., ... Thomson, S. I. (2018). Isca, v1.0: a framework for the global modelling of the atmospheres of earth and other planets at varying levels of complexity. *Geoscientific Model Development*, *11*(3), 843–859. doi: 10.5194/gmd-11-843-2018

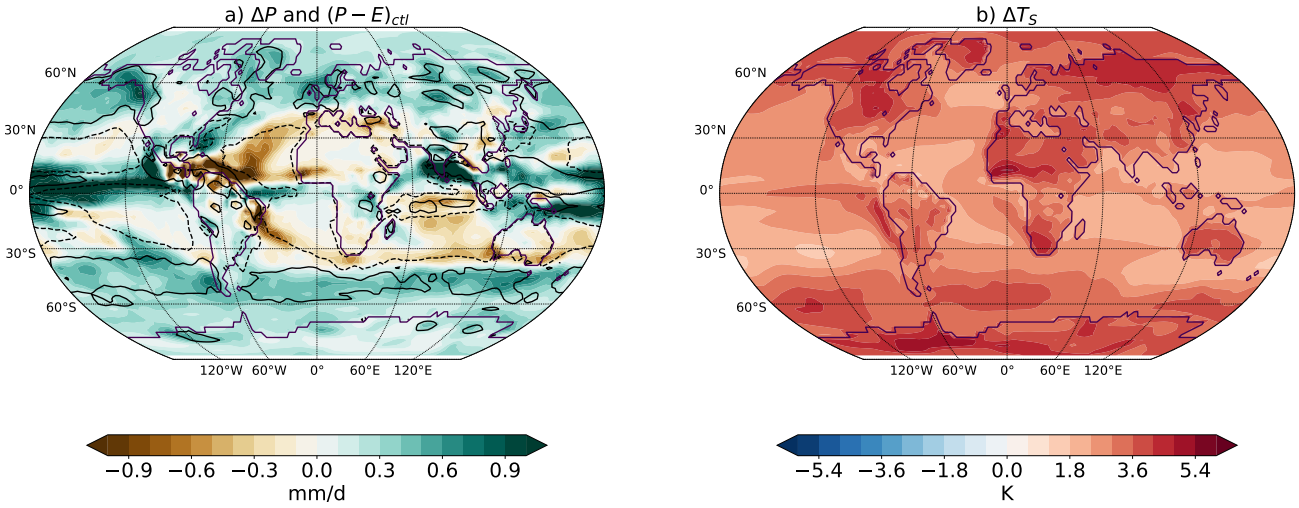

Figure S1. a) ΔP (colours) and $(P-E)_{ctl}$ (contours, -1.0 (dashed) and 1.0 (solid) mm/day) for the experiment with realistic continents and topography, but with parameterized ocean heat transport. b) Changes in surface temperatures (in K), clearly with a patterned ΔSST.

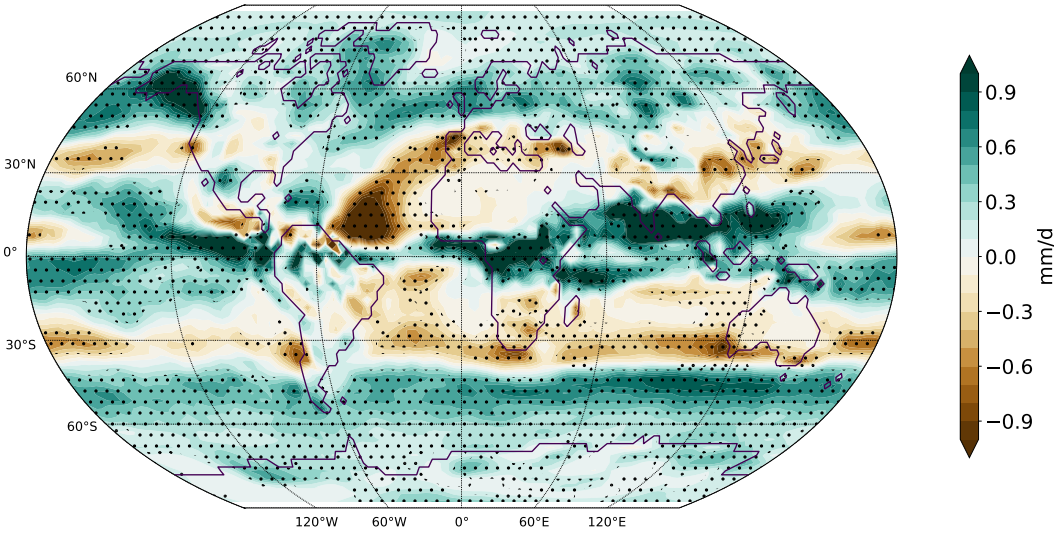

Figure S2. a) ΔP for experiment RC as in Fig. 1a from the main text. Areas in which ΔP exceeds the natural variability are stippled.

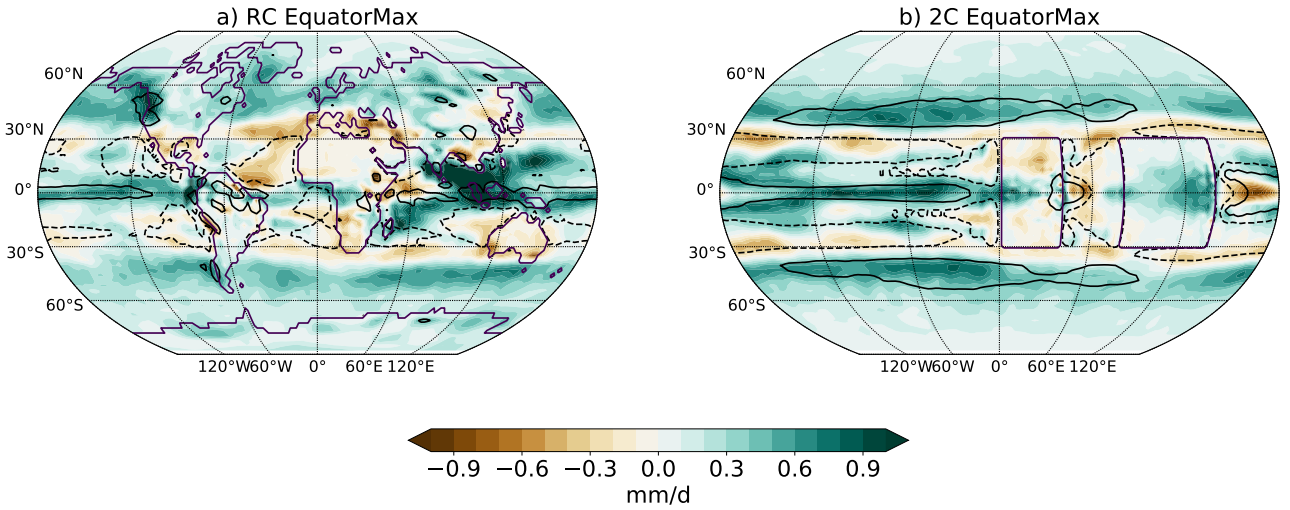

Figure S3. ΔP (colours) and $(P-E)_{ctl}$ (contours, -1.0 (dashed) and 1.0 (solid) mm/day) with the annual mean SST maximum located at the Equator instead of a few degrees North of the Equator for realistic continents with topography (a) and for the idealized two continents (b).

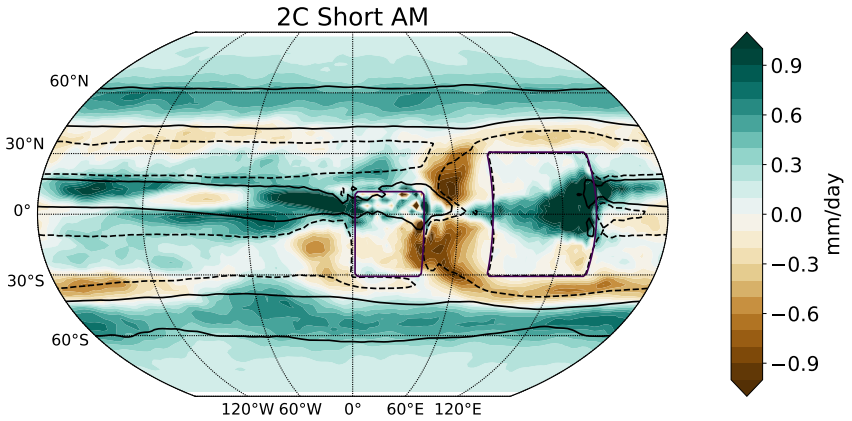

Figure S4. ΔP (colours) and $(P-E)_{ctl}$ (contours, -1.0 (dashed) and 1.0 (solid) mm/day) for a similar set-up as experiment 2C, but this time with a shorter latitudinal extent on the idealized American continent.

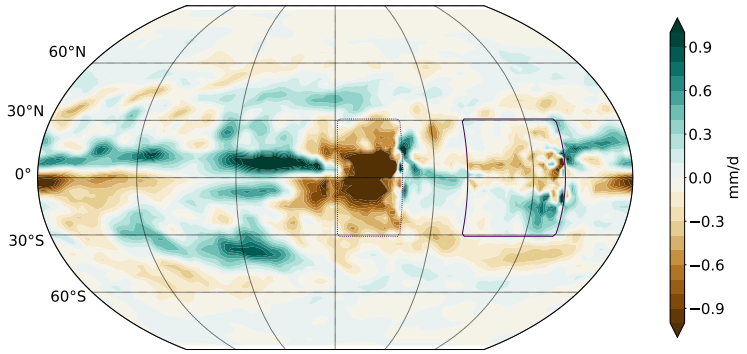

Figure S5. ΔP (colours) difference for the idealized continents (2C) minus Africa alone (AF), to show the influence of America (dashed contour) on Africa (solid contour).

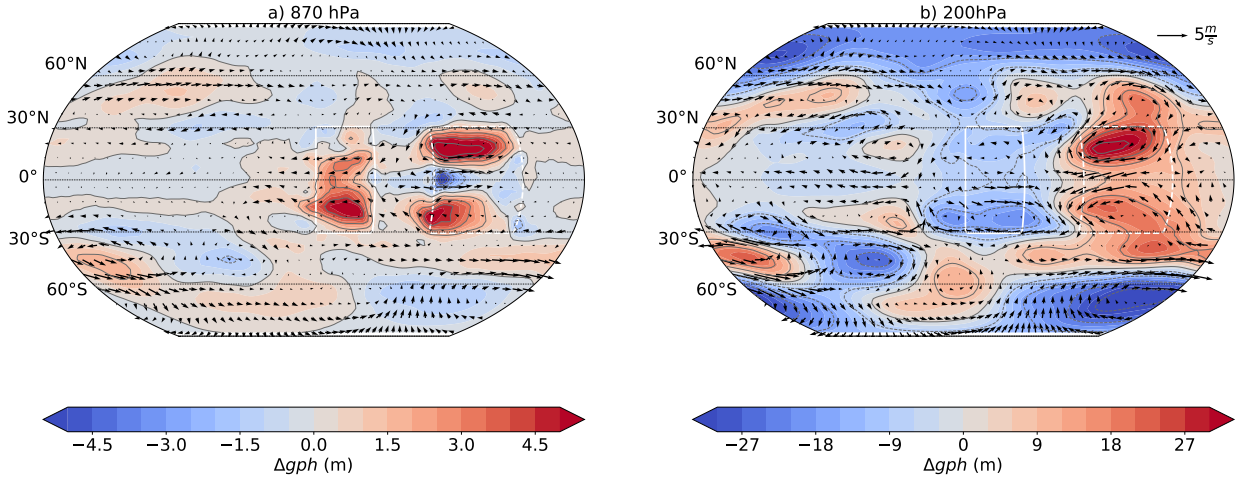

Figure S6. Warming-induced changes in the 870 hPa (a) and 200 hPa (b) geopotential height (colors and contours) for the 2C experiment minus AM. The vectors show the change in the horizontal wind field at the same pressure levels. The white contours show the position of the continents (solid for America which is present in both experiments, dotted for Africa which is only present in 2C but not in AM).

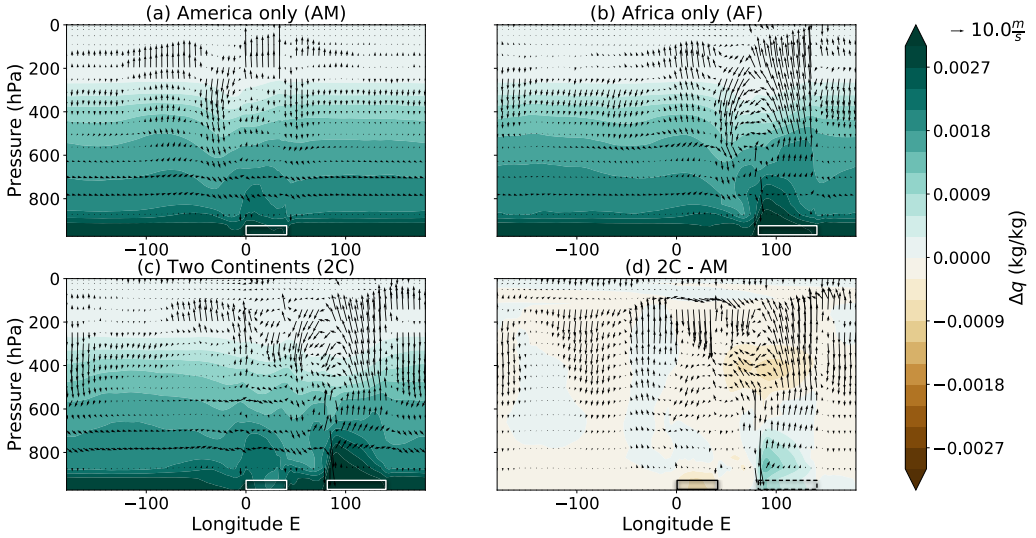

Figure S7. Warming-induced changes in q (colours, in kg/kg) and the zonal circulation (vectors, in m/s) averaged over 10°S - 10°N. The vectors are the same as in Figure 3 in the main text. The boxes show the locations of the idealized continents: a) America only (AM), b) Africa only (AF), c) Both continents (2C) and d) 2C - AM, where Africa is removed, thus its location is shown as a dashed box.

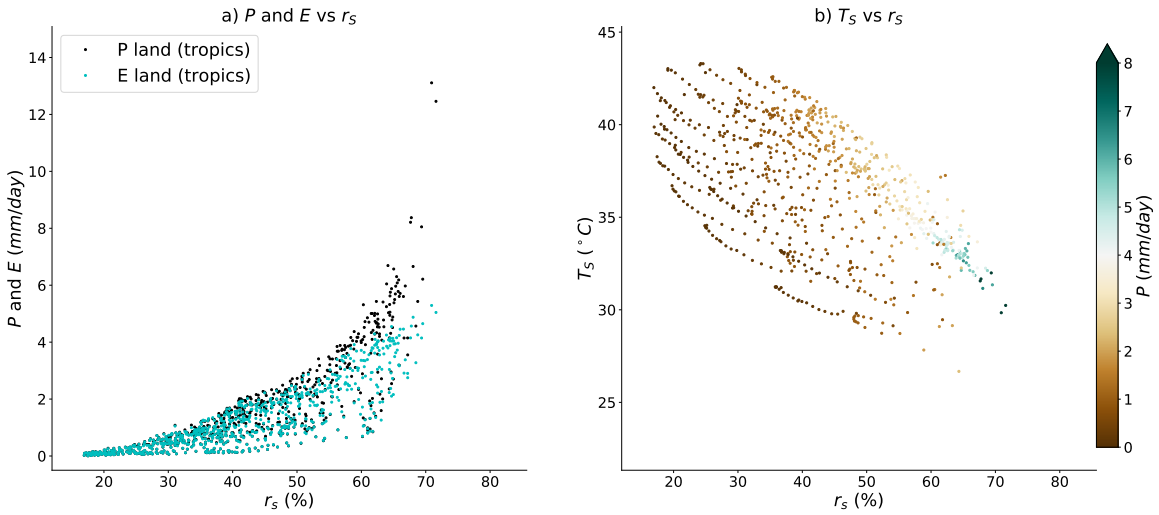

Figure S8. Relationship between a) P, E and r_s and b) T_S and r_S over tropical land derived from our two continents experiment (2C). The colours in (b) range from brown (little precipitation) to turquoise (a lot of precipitation).

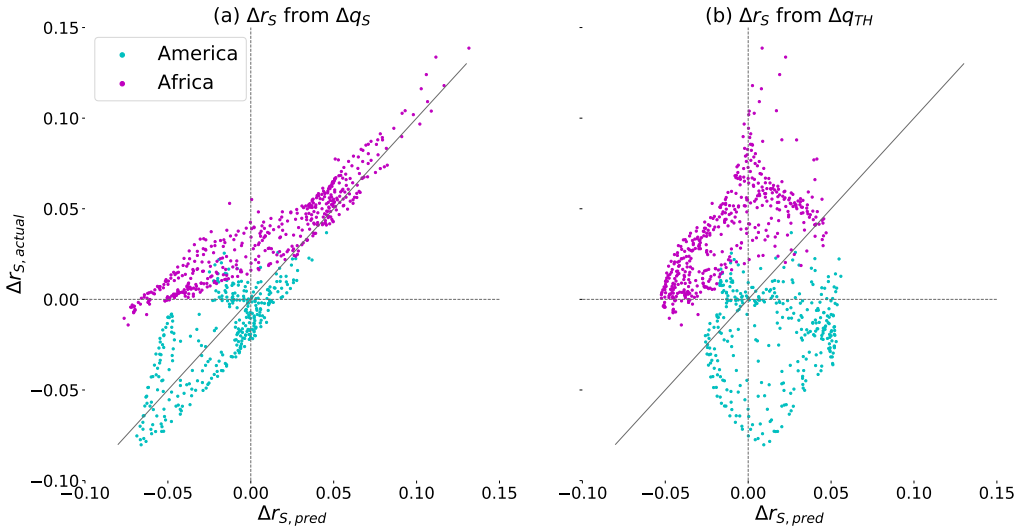

Figure S9. Predicted and actual Δr_S for each continent in our 2C experiment. Δr_S is predicted from Δq_S in (a) and from Δq_{TH} in (b). The solid line is $y = x$.